The infrared and ultraviolet spectra of single conformations of methyl-capped dipeptides: N-acetyl tryptophan amide and N-acetyl tryptophan methyl amide

Brian C. Dian, Asier Longarte, and Sebastien Mercier[a)]
Department of Chemistry, Purdue University, West Lafayette, Indiana 47907-1393

David A. Evans and David J. Wales
University Chemical Laboratories, Lensfield Road, Cambridge CB2 1EW, United Kingdom

Timothy S. Zwier[b)]
Department of Chemistry, Purdue University, West Lafayette, Indiana 47907-1393

(Received 30 July 2002; accepted 23 September 2002)

A combination of methods, including laser-induced fluorescence excitation, fluorescence-dip infrared (FDIR) spectroscopy, and UV-UV hole-burning spectroscopy, have been used to study the infrared and ultraviolet spectra of single conformations of two methyl-capped dipeptides: N-acetyl tryptophan amide (NATA) and N-acetyl tryptophan methyl amide (NATMA). Density functional theory calculations predict that all low-energy conformers of NATA and NATMA belong to one of two conformational families: C5, with its extended dipeptide backbone, or $C7_{eq}$, in which the dipeptide backbone forms a seven-membered ring joined by a H bond between the ψ-amide NH and the ϕ-amide carbonyl groups. In NATA (NATMA), the LIF spectrum has contributions from two (three) conformers. FDIR spectroscopy has been used to record infrared spectra of the individual conformers over the 2800–3600 cm^{-1} region, free from interference from one another. The NH stretch region provides unequivocal evidence that one of the conformers of NATA is C5, while the other is $C7_{eq}$. Similarly, in NATMA, there are two C5 conformers, and one $C7_{eq}$ structure. Several pieces of evidence are used to assign spectra to particular C5 and $C7_{eq}$ conformers. NATA(A) and NATMA(B) are both assigned as C5(AP) structures, NATA(B) and NATMA(C) are assigned as $C7_{eq}$ (ΦP), and NATMA(A) is assigned as C5(AΦ). In both molecules, the C5 structures have sharp vibronic spectra, while the $C7_{eq}$ conformers are characterized by a dense, highly congested spectrum involving long progressions that extend several hundred wave numbers to the red of the C5 S_1-S_0 origins. N-acetyl tryptophan ethyl ester (NATE), which can only form C5 conformers, shows only sharp transitions in its LIF spectrum due to four C5 conformers, with no evidence for the broad absorption due to $C7_{eq}$. This provides direct experimental evidence for the importance of the peptide backbone conformation in controlling the spectroscopic and photophysical properties of tryptophan. © *2002 American Institute of Physics.* [DOI: 10.1063/1.1521132]

I. INTRODUCTION

In order to understand the conformational preferences of flexible biomolecules, one must characterize an exponentially increasing number of conformational minima as the number of flexibility sites in the molecule grows. The most important regions of the potential energy surface are the lowest-energy minima, since it is there that the bulk of the population resides at thermal equilibrium. The number of thermally accessible minima may not grow at the same rate as the total number of conformational minima, and both theoretical[1,2] and experimental[3] studies have therefore typically focused attention on this low-energy region of the potential energy surface. From an experimental point of view, one would like to determine the number of conformational isomers present in a given sample, their structures, their relative populations, their spectroscopic signatures, and their response to solvent and other environmental parameters.

Recent studies are beginning to provide information of this type for small, flexible biomolecules in the gas phase.[4,5] By removing solvent effects and cooling the conformational population into low-lying conformational minima in a supersonic expansion, the innate conformational preferences of the isolated molecules can be probed, thereby providing a benchmark for calculations and a foundation for interpreting analogous data in solution. In the gas phase, the double resonance laser-based methods of UV-UV hole-burning, fluorescence-dip infrared spectroscopy, and resonant ion-dip infrared spectroscopy are capable of recording the ultraviolet and infrared spectra of individual conformations of flexible molecules free from interference from one another.[4,5] At the same time, increases in the speed and accuracy of calcula-

[a)]Permanent address: Laboratoire de chimie physique moléculaire (LCPM), École Polytechnique Fédérale de Lausanne (EPFL), CH-1015 Lausanne, Switzerland.
[b)]Author to whom correspondence should be addressed. Electronic mail: zwier@purdue.edu

 © 2002 American Institute of Physics

Downloaded 13 Jan 2003 to 131.111.112.171. Redistribution subject to AIP license or copyright, see http://ojps.aip.org/jcpo/jcpcr.jsp

tions are making it possible to predict low-energy minima and their spectroscopic properties for comparison with experiment.

In following this pathway from small to ever-larger, flexible biomolecules, recent gas-phase studies have begun to address molecules with several flexible sites.[6] Significant progress has been made in understanding the conformational preferences of individual amino acids (e.g., tryptophan and phenylalanine),[7] where several structures belonging to different conformational families have been observed and assigned. There, the ultraviolet chromophore in the amino acid (indole or benzene) provides the means of performing conformation-specific spectroscopy using the double-resonance methods mentioned in the preceding paragraph.

Tryptophan and phenylalanine-containing dipeptides represent a natural next step along the road to the study of even larger polypeptides. In the present paper, we present data on two methyl-capped dipeptides built off of tryptophan: N-acetyltryptophan amide (NATA) and N-acetyltryptophan methyl amide (NATMA), whose structures are shown below.

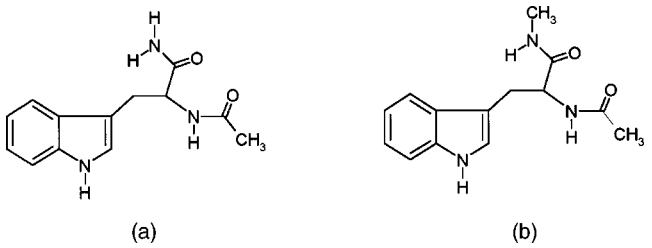

The methyl-capped dipeptides are better models for the polypeptide backbone (in which alkyl groups separate adjacent amide groups) than the unblocked dipeptides. As a result, methyl-capped dipeptides have served as model systems for both experimental and computational studies seeking to understand the first stages of polypeptide structure.[8–10]

Despite the rather modest proportions of these molecules relative to proteins, their study offers a venue for studying conformational preferences in a size regime where the full set of conformational minima can still be enumerated, but yet the complexity of the surface is sufficient to raise issues that will carry through to much larger systems. To illustrate this fact, Fig. 1 presents a disconnectivity graph[1,11] of NATMA's potential energy surface, produced with the AMBER force field.[12] The disconnectivity graph is a topological summary of the entire potential energy surface, with energy plotted along its vertical axis. The energies of individual conformational minima are represented as the ends of individual branches of the ''tree.'' Each node represents the energy at which the joined minima are mutually connected via one or more transition states. The exhaustive search that leads to the disconnectivity graph of Fig. 1 is feasible with a simple force field, but is of only approximate quantitative accuracy. On the other hand, a similar search using standard *ab initio* methods would be extremely time consuming, even at a modest level of theory. We shall see that the AMBER ''tree'' faithfully reproduces certain key aspects of the potential energy surface, and serves as a useful starting point for our discussion.

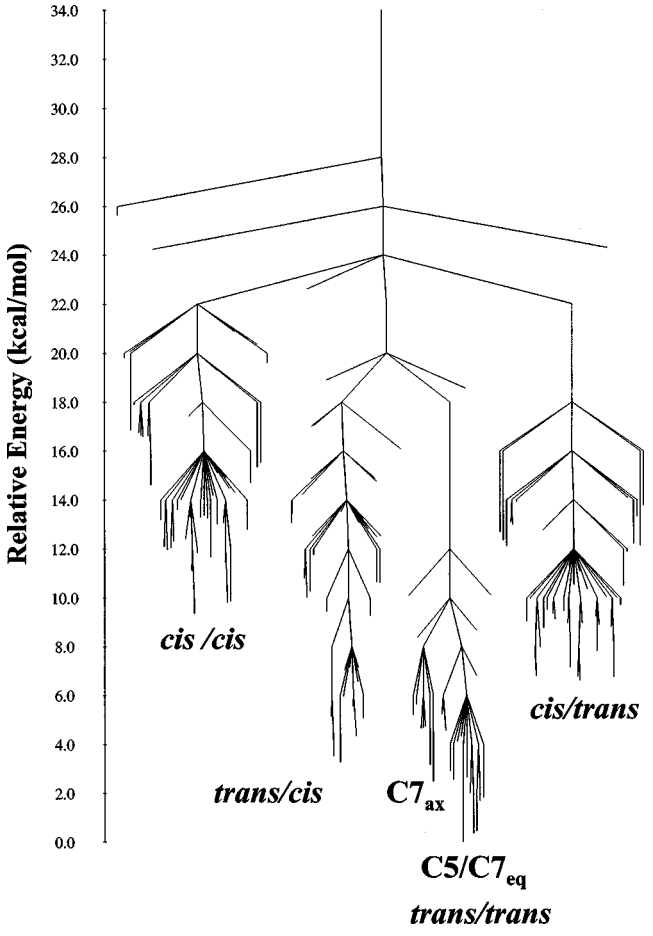

FIG. 1. Disconnectivity graph for N-acetyl tryptophan methyl amide (NATMA) using the AMBER force field. The energy scale is in kcal/mol relative to the global minimum. The end of each branch denotes the energy of a conformational minimum. Nodal points locate energies where transition states connect the minima, binned at 2 kcal/mol resolution. According to AMBER, there are 164 conformational minima and 714 transition states of NATMA.

According to the AMBER force field, NATMA has 164 conformational minima that are separated from one another by 714 transition states.[1] The disconnectivity graph separates into conformational basins associated with different families of conformational structures. Figure 2 shows examples of several of the conformational families labeled on the disconnectivity graph. Not surprisingly, the lowest-energy branch predicted by AMBER has two *trans*-amide peptide linkages. It is comprised of two structural types: C5 structures [Fig. 2(a)], with their extended (β-sheet-like) peptide backbone, and C7 structures in which the ψ-amide NH is H bonded to the ϕ amide carbonyl group, forming a seven-membered ring [equivalent to a γ turn, Figs. 2(b) and 2(c)]. In the $C7_{eq}$ ($C7_{ax}$) structures, the tryptophan side chain is in an equatorial (axial) position relative to the plane of the C7 ring. The other three major branches have ϕ-amide *cis*/ψ-amide *trans* [Fig. 2(d)], ϕ-*trans*/ψ-*cis* [Fig. 2(e)], and ϕ-*cis*/ψ-*cis* [Fig. 2(f)] structures, calculated to be about 4, 8, and 10 kcal/mol higher in energy, respectively, by the AMBER force field.

According to the AMBER force field, all of the low-energy structures are either C5 or $C7_{eq}$ structures. To the extent that this force field can serve as a guide, we anticipate

Downloaded 13 Jan 2003 to 131.111.112.171. Redistribution subject to AIP license or copyright, see http://ojps.aip.org/jcpo/jcpcr.jsp

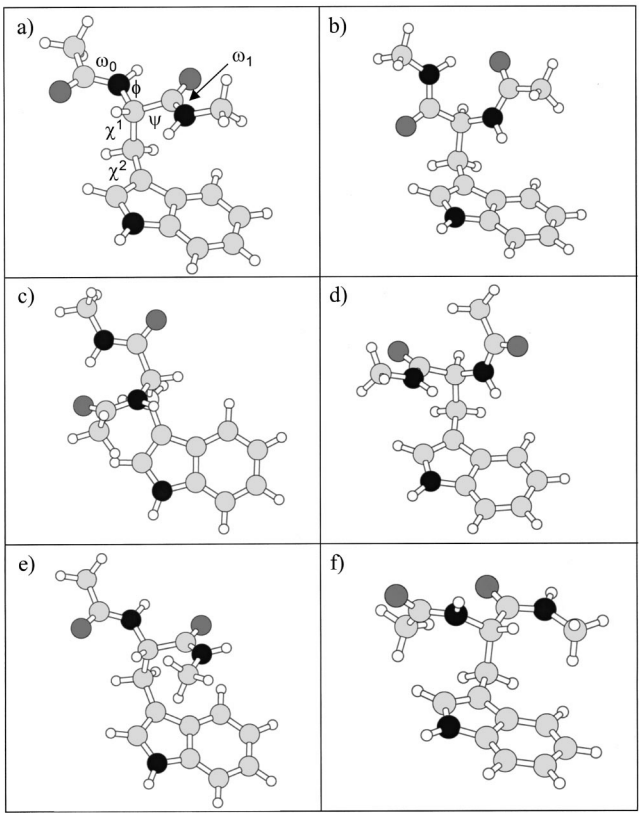

FIG. 2. (a) Structural diagram of a C5 structure of N-acetyl tryptophan amide (NATMA) with the flexible coordinates labeled. The ϕ and ψ angles are the same Ramachandran angles used to describe polypeptides. (b)–(f): Representative examples of the (b) $C7_{eq}$, (c) $C7_{ax}$, (d) ϕ *cis*-amide/ψ *trans*-amide, (e) ϕ *trans*-amide/ψ *cis*-amide, and (f) ϕ *cis*-amide/ψ *cis*-amide conformational families.

that conformers of both types may be present in the supersonic expansion, and could thereby be spectroscopically characterized both in the infrared and ultraviolet. That is the task of the present paper for NATA and NATMA.

The electronic spectroscopy of NATA has been studied previously under jet-cooled conditions by Tubergen *et al.*[13] These authors observed a single, sharp S_1-S_0 origin transition that is flanked by a weak, broad background with different emission characteristics. These different components of the spectrum were tentatively assigned to different conformations of NATA, but the nature of the conformations responsible for the two absorptions, and the reason for their different electronic spectroscopy were not determined in detail. NATMA has not been explored previously.

The electronic spectroscopy of indole and indole derivatives is complicated by the existence of more than one close lying excited state. In addition to the $^1\pi\pi^*$ state (labeled ^1L_b), which is the S_1 state in indole, there is a second $^1\pi\pi^*$ state, labeled ^1L_a, which in the gas-phase indole is $\sim$1200 cm^{-1} above ^1L_b.[14] It is well known from studies in solution that the ^1L_a state is lowered preferentially in polar solvents relative to ^1L_b, due to the much larger dipole moment of the former relative to the latter. By analogy, Levy and coworkers predicted that the side chain attached to the indole chromophore could influence the relative spacing of these two excited states in a similar way.[13]

In addition, the recent calculations of Sobolewski *et al.*[15] have identified a third excited singlet state that is nearby in energy, and could be very important to both the photophysics and photochemistry[16] of indole derivatives. This state is of $^1\pi\sigma^*$ character, has a very large dipole moment in the Franck–Condon region, and is dissociative along the indole NH bond. The existence and importance of this state have been recently highlighted by Dedonder-Lardeux *et al.*, who have shown that indole-$(NH_3)_n$ clusters undergo a hydrogen transfer reaction to form $NH_4(NH_3)_{n-1}$ radicals following photoexcitation in the ultraviolet.[17] No spectroscopic evidence has yet been provided for this state, nor for how it changes relative to ^1L_a and ^1L_b with changes in conformation or solvent type.

In this paper, we record ultraviolet and infrared spectra of single conformations of both NATA and NATMA. The comparison of the experimental IR spectra with the calculated vibrational frequencies and infrared intensities of individual conformers leads to assignments of the IR and UV spectra to individual conformers. There are two significantly populated conformers of NATA (one C5 and one $C7_{eq}$), and three of NATMA (two C5 and one $C7_{eq}$). In both molecules, it is the $C7_{eq}$ conformers that are responsible for the broad ''background'' absorption in the ultraviolet, while all C5 conformers produce sharp ultraviolet transitions. Thus, the present work provides spectroscopic evidence for the effect of the *conformation* of the side chain in both NATA and NATMA on the ultraviolet spectroscopy of these molecules.

II. METHODS

A. Experiment

The experimental apparatus used in these studies has been described in detail elsewhere[5] and only a brief description will be given here. NATA and NATMA were introduced into the gas phase by resistively heating the sample to approximately 175 °C in a sample holder located directly behind the pulsed valve. The samples were then expanded into vacuum via a pulsed valve (Parker General Valve, Series 9, 0.8 mm orifice, 20 Hz) using helium as a carrier gas with a backing pressure of 3 bar. Due to the thermally labile nature and low vapor pressures of NATA and NATMA at this temperature, flow rates on the order of 90–130 SCCM were used, which reduced the amount of decomposition that occurs prior to expansion. The high gas loads necessitated the evacuation of the chamber with a Roots blower (Leybold, WS1001).

A number of single and double resonance laser-based techniques were used to record infrared and ultraviolet spectra of single conformations of NATA and NATMA. UV laser pulses were generated by frequency doubling the output of a Nd:YAG pumped dye laser (rhodamine 590/610 mix, 20 Hz). A series of neutral density filters were used to reduce the output of visible light, yielding typical UV powers $<$500 μJ/pulse. The ultraviolet laser beam crosses the expansion approximately 5 mm downstream, where the total fluorescence is then monitored by a photomultiplier tube using a gated integrator.

One-color resonant two-photon ionization (R2PI) spectra

Downloaded 13 Jan 2003 to 131.111.112.171. Redistribution subject to AIP license or copyright, see http://ojps.aip.org/jcpo/jcpcr.jsp

were recorded to obtain spectra with mass resolution. UV laser pulses were generated by frequency doubling the output of a Nd:YAG pumped dye laser (rhodamine 590/610 mix, 20 Hz). Typical UV output was 0.5 mJ/pulse. Mass selection was achieved using linear time-of-flight methods.

Conformation-specific infrared spectra in the ground electronic state were obtained using fluorescence-dip infrared spectroscopy (FDIRS).[5,18] A seeded Nd:YAG pumped parametric converter (LaserVision, KTA based, 10 Hz), was used to produce tunable IR radiation from 2800–3600 cm^{-1}. Infrared laser powers of 1–5 mJ/pulse were typical. The UV and IR laser beams are spatially overlapped approximately 5 mm from the pulsed valve, and temporally separated by approximately 100 ns, with the IR preceding the UV. To generate the FDIRS spectrum, the UV laser is fixed to a particular vibronic transition in the LIF spectrum and the total fluorescence signal is monitored. Whenever the parametric converter is resonant with an infrared transition in the tuning range 2800–3600 cm^{-1}, the population is removed from the ground vibrational state, which results in a depletion in the total fluorescence signal from that level when the UV laser interrogates it. Depletions are recorded by comparing the total fluorescence signal with and without the IR laser present using active baseline subtraction in a gated integrator (Stanford Research Systems) interfaced with a personal computer.

UV–UV hole-burning spectroscopy was used to record the ultraviolet spectra of single conformers in the expansion. To do so, a higher-power hole-burn laser is fixed on a specific vibronic transition in the UV. The probe laser is then turned over the region of interest, and hole-burning spectra are recorded by monitoring the difference in the LIF signal when the pump UV beam is ''on'' versus ''off'' via active baseline subtraction. Because the pump laser is fixed to a single transition, all peaks that originate from the same ground state in the UV spectrum appear as depletions in the total fluorescence signal. In this work, both the FDIR and hole-burning spectra are plotted as negative-going peaks because they represent depletions in the total fluorescence signal.

NATA was used as purchased from Aldrich Chemical Company. NATMA was synthesized by the technique outlined by Souhassou *et al.*[19] To perform the synthesis, two grams of *n*-acetyltryptophan ethyl ester (Aldrich) was dissolved in 30 mL of dry methanol. Approximately 50 equivalents of methyl amide in ethanol was added to the solution and allowed to react under a nitrogen atmosphere in excess of twenty-four hours. Thin-layer chromatography (silica support; 9:1 $CHCl_3$:MeOH mobile phase) was run, comparing the starting product with reactants to determine the extent of completion of the reaction. After the reaction was complete, the excess solvent was evaporated, and the product was recrystallized and filtered in a 1:1 mixture of cold ethanol/hexane. Purity of the product was confirmed by NMR analysis and laser-induced fluorescence spectroscopy.

B. Theoretical

Due to the large size and multiple flexible coordinates of the molecules studied herein, a simple conformational search based on intuitively rotating about bond torsions runs a substantial risk of missing structures. Since high-level calculations are computationally expensive, it is desirable to have an efficient method of screening for low-energy conformers, which could then be used as input for *ab initio* or density functional theory (DFT) calculations using the GAUSSIAN 98 suite of programs.[20] The conformational searching algorithm in the molecular mechanics package MacroModel[21] was used for this purpose. Preliminary searches used multiple force fields (MM2,[22] MM3,[23] MMFF, MMFFs,[24] OPLS-A, and OPLS-AA[25]), so that the results could be compared with one another. The reliability of these force fields for predicting quantum chemical relative energies of alanine di- and tetrapeptides in various regions of conformational space has been tested by Beachy *et al.*,[8] and will not be discussed further here. Slight variations in the searching procedure for each molecule are detailed below.

As Beachy *et al.* suggest,[8] the OPLS-AA force field[25] produced results that most accurately reflected the DFT results for the molecules studied here. OPLS-AA geometries within 5 kcal/mol of the global minimum were used as starting geometries for DFT calculations employing the Becke3LYP functional[26] with a 6-31+G* basis set.[27] The DFT calculations represented a reasonable compromise between accuracy and speed for molecules of this size, with 18 or 19 heavy atoms. Harmonic vibrational frequency calculations and infrared intensities were calculated at the same level of theory for comparison with the experimental results. A scaling factor of 0.9605 was applied to the harmonic results in order to bring the indole NH stretch fundamental into agreement with experimental results.[28] Conformational minima were confirmed by the absence of imaginary frequencies in the vibrational calculations. The vibrational frequency calculations are then compared to experimental spectra, and serve as a basis for making conformational assignments.

III. RESULTS AND ANALYSIS

A. Calculated structures, energetics, and vibrational frequencies

Figure 2(a) shows a low-energy C5 conformer of NATMA that highlights the torsional angles varied during conformational searches. In all the searches, the torsions of particular interest are the Ramachandran angles ϕ and ψ associated with the dipeptide backbone.[29] As indicated earlier, most of the low-energy structures belong to one of two peptide backbone conformations, labeled as C5 and $C7_{eq}$ [Figs. 2(a) and 2(b)]. These structures have also been identified as the lowest-energy structures found in gas-phase calculations on di- and tetra-peptide analogs of glycine and alanine.[9]

In addition to the Ramachandran angles ϕ and ψ, the N-acetyl and amide (methylamide) groups can take up different positions with respect to the indole ring. We have adopted a notation that builds on the previous labeling scheme used on tryptamine[6] that enables the succinct identi-

Downloaded 13 Jan 2003 to 131.111.112.171. Redistribution subject to AIP license or copyright, see http://ojps.aip.org/jcpo/jcpcr.jsp

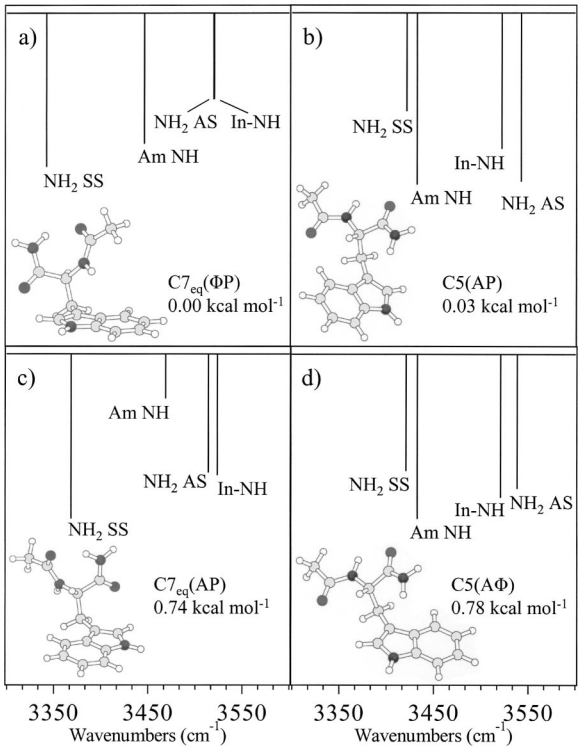

FIG. 3. Structures, labels, and relative energies of the four lowest-energy conformations of NATA calculated at the DFT/B3LYP 6-31+G* level of theory.

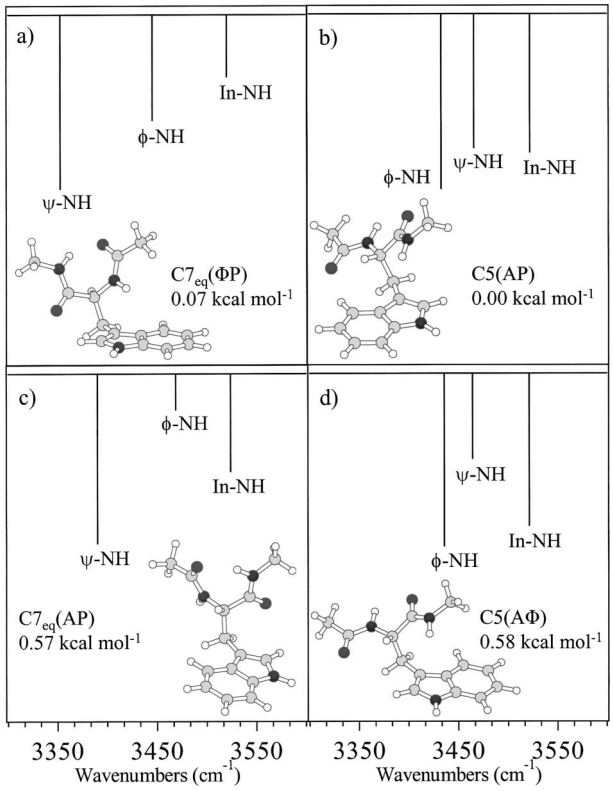

FIG. 4. Structures, labels, and relative energies of the four lowest-energy conformations of NATMA calculated at the DFT/B3LYP 6-31+G* level of theory. Note the close similarity with Fig. 3, indicating that the additional methyl group is not calculated to have a significant effect on the relative conformational energies.

fication of all the conformers presented in this work. The designation Cn(XY), uses the Cn term to refer to either the C5 or C7 geometry, where the C7 will be followed by a subscript ''ax'' or ''eq'' to denote either the axial or equatorial position of the $C_\alpha - C_\beta$ bond relative to the plane of the C7 ring. The X term refers to the position of the N-acetyl group (ϕ bond), and Y to the position of the ψ amide group relative to the indole ring. X and Y can have the value A, P and Φ, where A denotes anti with respect to the indole ring, P denotes gauche on the pyrrole side of indole, and Φ denotes gauche on the phenyl side of the indole ring. Thus, the term $C7_{eq}(AP)$ would indicate a C7 equatorial peptide backbone with the phi bond ''anti'' to the indole ring and the psi bond gauche to the indole ring on the pyrrole side of indole.

The success of the force fields in identifying the global conformational minima varies significantly. The results of the search found OPLS-AA[25] to most accurately predict the low-lying conformations with respect to DFT calculations [no zero-point energy (ZPE) correction] for both NATA and NATMA. Other force fields had significant error in the relative energies of the conformers or, as in the case of MM3, missed low-lying conformers altogether. Of the 12 OPLS-AA geometries optimized by DFT, 4 low-lying conformations (<1 kcal/mol after ZPE correction) were found for NATA and are shown in Fig. 3. The calculations separate these four into two pairs, each having a C5 and $C7_{eq}$ structure, each pair energetically separated by about 0.7 kcal/mol. The DFT calculations place the $C7_{eq}(\Phi P)$ as the lowest-energy conformation, with C5(AP) being only 0.03 kcal/mol higher in energy after ZPE. The next two structures are $C7_{eq}(AP)$ and $C5(A\Phi)$, which are 0.74 and 0.78 kcal/mol, respectively, above the global minimum.

The analogous conformational search on NATMA, with its methyl substitution on the amide group, produces geometries and energetics for the low-lying minima that closely mimic those of NATA. Similarly, the DFT calculations predict that the same four low-lying minima (<1 kcal/mol from the lowest-energy conformer) found for NATA are also the lowest-energy structures for NATMA. These structures and their relative energies are shown in Fig. 4.

Calculations of the vibrational frequencies and infrared intensities of several of the low-lying C5 and C7 conformations of both NATA and NATMA have been carried out. NATA has four NH stretches that give rise to four transitions in the infrared: indole NH, ϕ-amide NH, and two ψ-amide NH stretches from the NH_2 group. In NATMA, one of the ψ-amide NH_2 hydrogens is replaced by a methyl group, reducing the total number of NH stretch vibrations from four to three. The hydride stretch frequencies and intensities of the four lowest-energy structures of NATA and NATMA are collected in Table I, together with their assignments. The NH stretch frequencies and IR intensities are also shown as stick diagrams in Figs. 3 and 4, respectively. The stick spectra show that the C5 and C7 families have distinct amide NH stretch spectra that can be used to identify them unambiguously. In the C7 structures of NATMA [Figs. 4(a) and 4(c)], the ψ-amide NH is involved in a H-bond with the N-acetyl carbonyl group. This lowers the frequency of the ψ-amide

Downloaded 13 Jan 2003 to 131.111.112.171. Redistribution subject to AIP license or copyright, see http://ojps.aip.org/jcpo/jcpcr.jsp

TABLE I. Experimental vibrational frequencies and proposed assignments of the NH stretch vibrations of NATA and NATMA.

	NATA(A) C5	NATA(B) $C7_{eq}$	NATMA(A) C5	NATMA(B) C5	NATMA(C) $C7_{eq}$
ϕ-amide NH	3430	3429	3440	3431	3429
ψ-amide NH_2	3417	3334			
ψ-amide NH_2	3538	3516			
ψ-amide NH			3466	3454	3344
Indole NH	3523	3521	3522	3522	3523

NH stretch fundamental by about 80 cm^{-1}, and increases its intensity by about a factor of 3 from that in the C5 conformers [Figs. 4(b) and 4(d)]. Similarly, in NATA, the NH_2 stretching modes change from symmetric and antisymmetric stretches at about 3420 and 3540 cm^{-1} in the C5 conformers [Figs. 3(b) and 3(d)] to partially localized H-bonded NH and free NH stretches with frequencies near 3335 and 3520 cm^{-1} in the $C7_{eq}$ conformers [Figs. 3(a) and 3(c)].

The calculated CH stretch vibrations of NATA and NATMA include the pyrrole CH (calculated to be very weak, appearing at 3150 cm^{-1}), four aromatic CH stretches in the 3050–3100 cm^{-1} region, and the alkyl CH stretches [due to C_α and C_β methylene and the methyl group(s)] between 2850 and 3000 cm^{-1}. These regions are both highly congested and subject (experimentally) to Fermi resonance mixing with overtones of the CH bends. Nevertheless, there are subtle differences in the calculated CH stretch fundamentals with conformation that turn out to play a supporting role in the assignment process that follows.

B. LIF and UV–UV hole burning

1. NATA

The LIF spectrum of NATA in the origin region is shown in Fig. 5(a). The peaks labeled DP(1)–DP(3) are transitions ascribable to a thermal decomposition product of NATA. Qualitative assignment as a decomposition product could be made simply on the basis of the growth of these transitions when the sample was heated to temperatures above 175 °C, and their retention when the temperature was subsequently reduced. In order to determine the nature of the decomposition product, R2PI scans were recorded while monitoring the NATA parent mass (245 amu) and other mass channels, including mass 227, corresponding to the loss of water. The R2PI scan of the $m/z=227$ channel, shown as an inset in Fig. 5(a), shows that the peaks DP(1)–DP(3) are all due to a decomposition product involving the loss of water. It was found that using flow rates of 90–130 SCCM and restricting sample temperatures to <175 °C helped reduce its formation.

The R2PI scan of NATA (not shown) identifies the rest of the transitions in Fig. 5(a) as arising from the NATA monomer. In particular, a single, dominant origin transition appears at 34 961 cm^{-1} (labeled A), while a weak, broad background (labeled B), just barely discernable in Fig. 5(a), extends to the red of this origin. These features of the spectrum are qualitatively similar to those found by Tubergen *et al.*[13] However, their LIF spectrum has no detectable contribution from the decomposition product. We note that Tubergen *et al.*[13] used a continuous flow expansion, while ours is pulsed. We postulate that a continuous flow expansion may minimize the mechanism that leads to decomposition, possibly by reducing the amount of time *gas-phase* molecules are exposed to the pre-nozzle temperature.

UV–UV hole-burning spectra of NATA are shown in Figs. 5(b) and 5(c). In order to enhance the signal of the peaks due to the red-shifted progression, the probe laser was focused with a 50 cm lens, thereby partially saturating these transitions. The hole-burning spectra of Figs. 5(b) and 5(c)

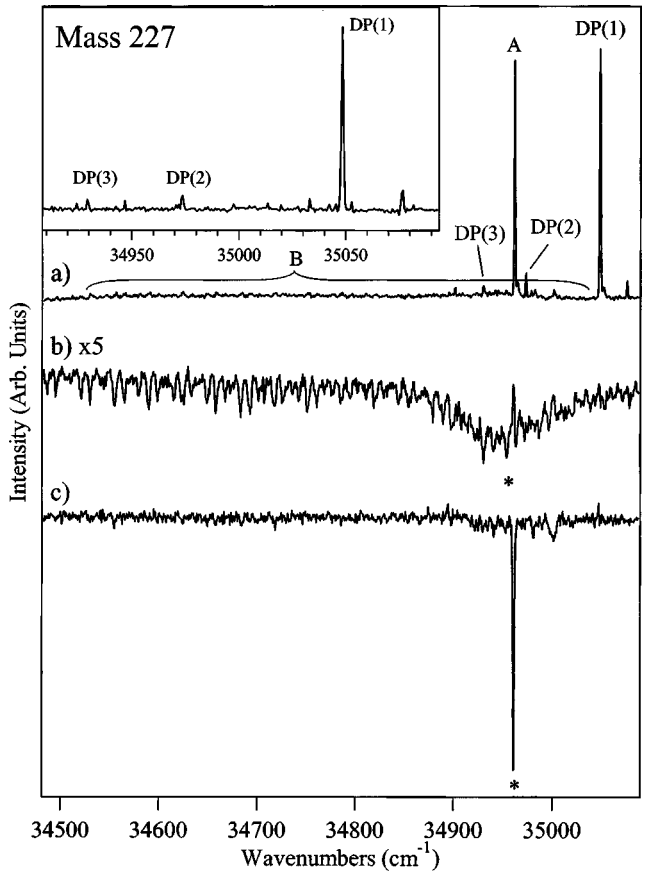

FIG. 5. (a) The LIF excitation spectrum of NATA cooled in a supersonic expansion, taken over the region near the S_0-S_1 origin. The transitions labeled DP(n) are those of a thermal decomposition product. The inset shows an R2PI spectrum of the decomposition product, taken at $m/z=227$, involving the loss of water from NATA. (b) UV–UV hole-burning spectrum with hole-burn laser fixed at 34 945 cm^{-1}, indicated by the asterisk. (c) Analogous hole-burning spectrum with the hole-burn laser fixed on transition A at 34 961 cm^{-1}. The hole-burn spectra prove that the LIF spectrum is composed of two conformers of NATA. See the text for a further discussion.

Downloaded 13 Jan 2003 to 131.111.112.171. Redistribution subject to AIP license or copyright, see http://ojps.aip.org/jcpo/jcpcr.jsp

were taken with the hole-burn laser fixed at 34 945 cm^{-1} (corresponding to the background progression) and transition A (34 961 cm^{-1}), respectively, while the probe laser was tuned over the region 34 780–35 090 cm^{-1}.

As expected, the hole-burning spectrum in Fig. 5(c) reveals a dominant origin transition A, and a weak vibronic structure built off of it. The spectrum of Fig. 5(b) is much more surprising. The most intense part of the spectrum appears near origin A, but consists of a dense clump of transitions spread over some 50 cm^{-1} rather than a single sharp transition. Furthermore, the dense vibronic structure continues to the red of 34 900 cm^{-1}, extending to 34 500 cm^{-1} and beyond. Tubergen *et al.* have followed this structure down to 34 375 cm^{-1}.[13] Multiple attempts to identify contributions due to different conformations within the broad progression were made by positioning the hole-burn laser at different frequencies in the UV. In every case, all the structure vibronic of Fig. 5(b) burned together, demonstrating that it is all from a single ground state conformer. Thus, there are two conformers of NATA present in the expansion: conformer A with its sharp vibronic spectrum, and conformer B, with its dense, widely spread, red-shifted vibronic structure.

2. NATMA

The LIF spectrum of NATMA in its origin region is shown in Fig. 6(a), in which several prominent features appear. Even though the addition of a methyl group is predicted by the calculations to have little bearing on the preferred structures and relative energies of the conformers of NATA and NATMA, this small change in structure induces striking differences in the spectroscopy of the two molecules. The peak at 35 029 cm^{-1} (labeled DP) is again attributed to a decomposition product that significantly increases in intensity as the temperature is raised above 175 °C. The mass-selected R2PI spectrum (not shown) confirms that the peak at 35 029 cm^{-1} is due to decomposition, where the mass of the decomposition product corresponds once again to loss of 18 amu from NATMA. In addition to the main decomposition peak, there are three minor peaks to the red of this band that are also due to the decomposition product, occurring at 34 945, 34 960 and 34 975 cm^{-1}.

Two Franck–Condon progressions are immediately obvious in the LIF spectrum, labeled A and B in Fig. 6(a). Progression A extends over three members, which have a 24 cm^{-1} spacing. It is shifted farthest to the red, with its first member appearing at 34 881 cm^{-1}. Progression B is carried over five peaks, which have a 12 cm^{-1} spacing. This progression has its first member at 34 913 cm^{-1}. Less obvious, but altogether similar to NATA, a background is present under the set of sharp transitions. However, unlike NATA, this background is weaker and shows a less well-resolved structure to the red of the sharp transitions.

The UV–UV hole-burning spectra of NATMA are presented in Figs. 6(b) and 6(d). The asterisks in the figure mark the UV wavelength where the hole-burning laser was fixed for each of the spectra. The spectra of Figs. 6(c) and 6(d) demonstrate that the two major progressions of A and B originate from two distinct conformers, with the transition at 34 881 cm^{-1} the $S_1 \leftarrow S_0$ origin of conformer A, and the transition at 34 913 cm^{-1} the origin of conformer B. Additionally, as in the case of NATA, the ''background'' burns separately from the other two conformations, and is ascribable entirely to a third conformer of NATMA with completely different electronic spectroscopy than the other two. In what follows, we will label this third conformer as ''conformer C.'' The assignment of these three (two) contributions to the UV spectrum to conformers of the NATMA (NATA) monomer is consistent with their presence in the R2PI spectra in the monomer mass channel, but also will be confirmed by the FDIR spectra of the next section.

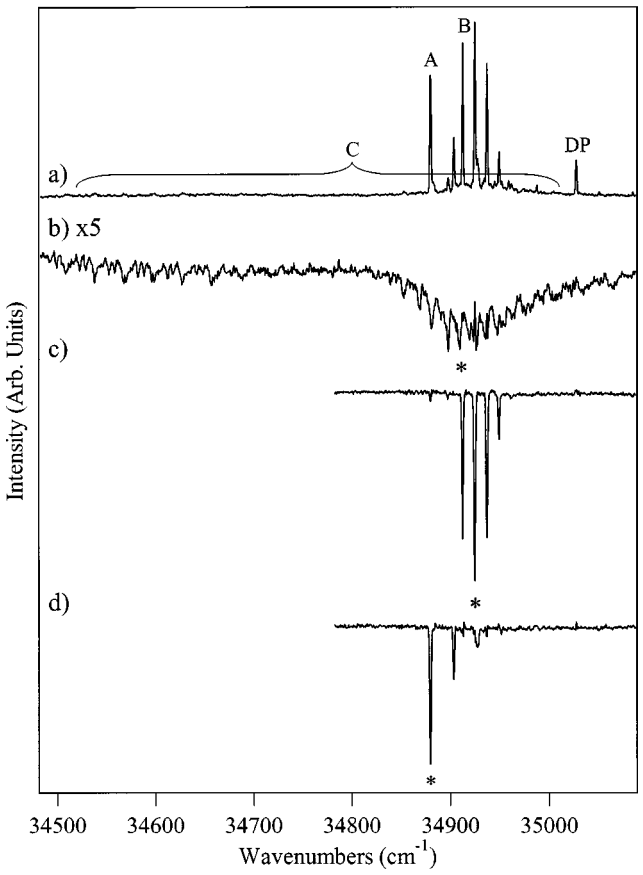

FIG. 6. (a) The LIF excitation spectrum of NATMA cooled in a supersonic expansion, taken over the region near the S_0–S_1 origin. The transitions labeled DP(n) are those of a thermal decomposition product. (b)–(d) UV–UV hole-burning spectra taken with a hole-burn laser fixed at (b) 34 903 cm^{-1}, (c) 34 913 cm^{-1}, and (d) 34 881 cm^{-1}, respectively, indicated by asterisks. The hole-burn spectra prove that the LIF spectrum is composed of three conformers of NATMA. See the text for a further discussion.

C. FDIR spectra

FDIR spectra of NATA conformers A and B in the hydride stretch region (2800–3600 cm^{-1}) are shown in Fig. 7(a) and 7(c), respectively. These spectra were taken by fixing the UV on the origin transition of NATA(A) (34 961 cm^{-1}) and at 34 945 cm^{-1}, in the dense structure attributed to NATA(B). The two spectra are clearly different from one another, most noticeably in the NH stretch region. The experimental frequencies and their vibrational assignments are summarized in Table II. Both spectra have four NH stretch fundamentals [two of which are nearly overlapped at 3518

Downloaded 13 Jan 2003 to 131.111.112.171. Redistribution subject to AIP license or copyright, see http://ojps.aip.org/jcpo/jcpcr.jsp

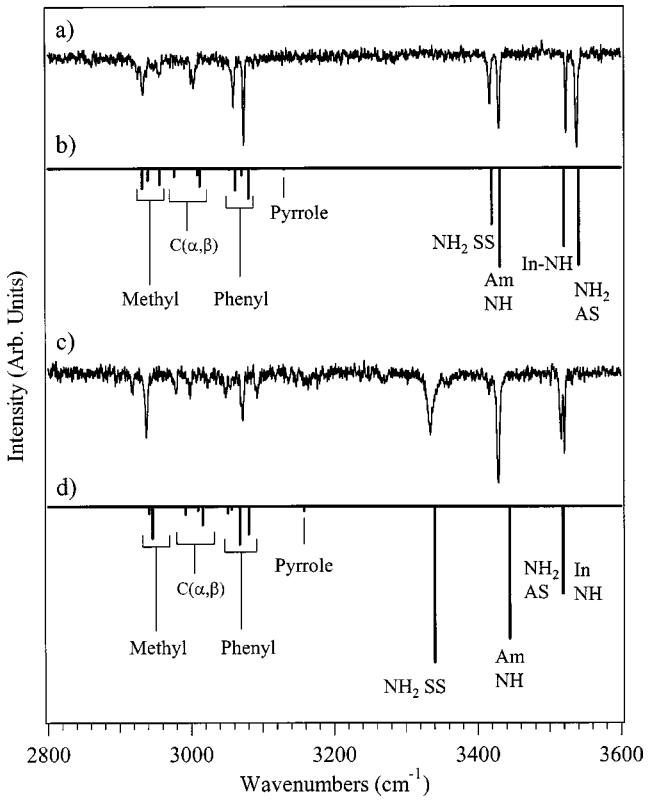

FIG. 7. Hydride stretch FDIR spectra of conformers (a) A and (c) B of NATA. In recording these spectra, the LIF probe laser was fixed at wavelengths corresponding to the asterisks in Fig. 5. (b) and (d) Stick diagram showing the harmonic vibrational frequencies and infrared intensities calculated for the (b) C5(AP) and (d) $C7_{eq}(\Phi P)$ structures. The frequencies have been scaled by 0.9605 to align the indole NH stretch fundamentals with experiment.

cm^{-1} in NATA(B)], consistent with their assignment to two conformers of the NATA monomer. The four bands appear as two sets of doublets in NATA(A) (at 3417/3430 and 3523/3538), while in NATA(B), one of the bands is shifted all the way down to 3334 cm^{-1} and is significantly broadened compared to the other bands. Both these characteristics of the 3334 cm^{-1} fundamental suggest that the NH group responsible for this absorption is involved in a H bond. Based on the calculations (Fig. 3), this suggests that NATA(B) is a C7 conformer, with an intramolecular H bond between one of the ψ-amide NH's and the ϕ-amide carbonyl group.

The indole NH stretch appears at 3523 cm^{-1} in NATA(A) and 3521 cm^{-1} in NATA(B). This is very close to its frequency in the indole monomer (3525 cm^{-1}). This band is also unusually and characteristically sharp, helping in its identification. Not surprisingly, the different conformations of the dipeptide backbone have little bearing on the frequency of this fundamental.

The corresponding spectra of the three conformers of NATMA are shown in Figs. 8(a), 8(c), and 8(e). Here, the substitution of one of the ψ-amide NH groups with a methyl group reduces the number of NH stretch fundamentals from four to three, as anticipated. As in NATA, the indole NH stretch fundamentals appear within a wave number or two of each other, and appear as isolated bands on the high-frequency end of the spectrum. The NATMA (A) and (B) spectra have very similar spectral patterns, suggesting that they arise from the same conformational family. On the other hand, NATMA(C) has amide NH stretch fundamentals appearing at 3344 and 3429 cm^{-1}, very similar to the 3334 and 3429 cm^{-1} transitions in NATA(B). The 3344 cm^{-1} band also possesses a similar breadth and increased integrated intensity to its NATA(B) counterpart, indicative of an intramolecular H bond. We surmise on this basis that NATMA(C), like NATA(B), is a C7 conformer.

Immediately below the experimental spectra of Fig. 7 and Fig. 8 are calculated hydride stretch infrared spectra for individual C5 and $C7_{eq}$ conformers of NATA and NATMA. Arguments will be made shortly for an assignment of the experimental spectra to specific C5 and $C7_{eq}$ conformers.

TABLE II. A comparison of the calculated and experimental hydride stretch vibrational frequencies and infrared intensities of the two observed conformers of NATA.

	NATA A				NATA B			
	Experimental frequency	Calculated frequency C5(AP)	Experimental intensity	Calculated intensity C5(AP)	Experimental frequency	Calculated frequency $C7_{eq}(\Phi P)$	Experimental intensity	Calculated intensity $C7_{eq}(\Phi P)$
Alkyl CH	2933	2932	0.43	0.20	2919	2935	0.15	0.04
		2940		0.12		2941		0.05
	2956	2956	0.24	0.16	2938	2946	0.51	0.21
		2977		0.08	2979	2992	0.14	0.05
		3009		0.07		3009		0.03
	3004	3012	0.35	0.18	2999	3016	0.19	0.12
Phenyl CH		3054		0.01	3048	3051	0.18	0.04
	3059	3062	0.57	0.22		3057		0.02
		3071		0.07	3072	3068	0.36	0.25
	3074	3081	0.97	0.31	3092	3080	0.18	0.18
Pyrrole CH		3130		0.01		3158		0.03
NH stretch	3417	3420	0.53	0.57	3334	3340	0.59	1.00
	3430	3431	0.80	1.00	3429	3444	1.00	0.85
	3523	3520	0.85	0.79	3516	3518	0.63	0.56
	3538	3541	1.00	0.98	3521	3519	0.74	0.58

Downloaded 13 Jan 2003 to 131.111.112.171. Redistribution subject to AIP license or copyright, see http://ojps.aip.org/jcpo/jcpcr.jsp

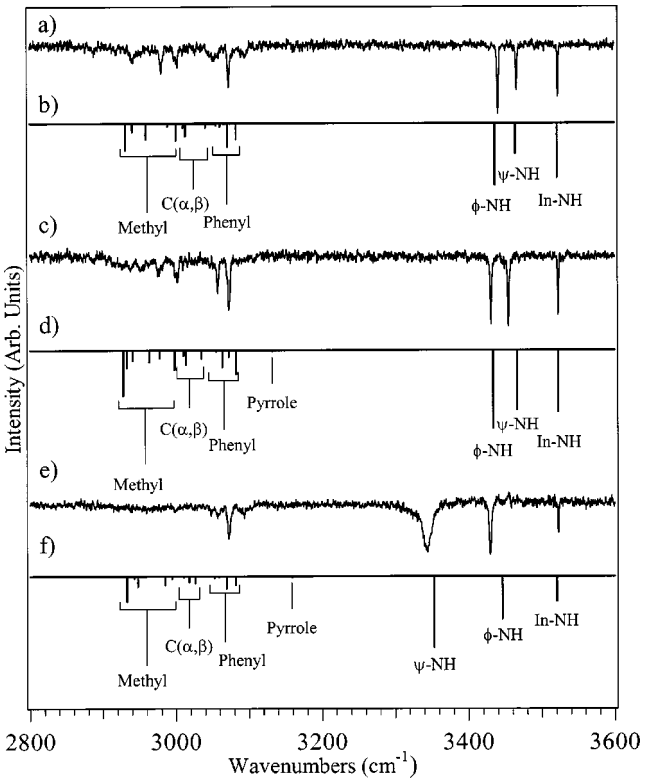

FIG. 8. Hydride stretch FDIR spectra of conformers (a) A, (c) B, and (e) C of NATMA. In recording these spectra, the LIF probe laser was fixed at wavelengths corresponding to the asterisks in Fig. 6. (b), (d), and (f). Stick diagram showing the harmonic vibrational frequencies and infrared intensities calculated for the (b) C5(AΦ), (d) C5(AP), and (f) $C7_{eq}$(ΦP) structures. The frequencies have been scaled by 0.9605 to align the indole NH stretch fundamentals with experiment.

Initially, however, we use them simply to confirm assignments to conformational families.

As anticipated already, visual inspection of the experimental spectra of Figs. 7(a) and 7(c) with the calculated spectra of Figs. 7(b) and 7(d) confirms that NATA(A) is a C5 conformer, while NATA(B) is a $C7_{eq}$ structure. The calculated and experimental spectra show a characteristic pair of doublets for the C5 NH stretches, and an intense band with a large frequency shift due to the intramolecular ϕ-amide NH H bond in the $C7_{eq}$ spectrum.

Similarly, in NATMA, the calculated spectra for the C5 conformers of Figs. 8(b) and 8(d) compare favorably with the experimental spectra of NATMA(A) [Fig. 8(a)] and NATMA(B) [Fig. 8(c)], while the corresponding calculations for the $C7_{eq}$ conformers [Fig. 8(f)] reproduce the experimental spectrum of Fig. 8(e). This confirms our assignment of NATMA(A, B) to C5 structures, and NATMA(C) to a $C7_{eq}$ structure.

The characteristic patterns of the C5 and $C7_{eq}$ NH stretch fundamentals enable the assignment of individual transitions in these spectra to specific NH stretch normal modes. As labeled in the figure, it is the ψ-amide NH group that is involved in the intramolecular H bond in the $C7_{eq}$ structures of NATA(B) and NATMA(C). The H bond lowers the frequency of this band (3334 and 3344 cm^{-1}, respectively), increases its intensity, broadens the transition, and localizes the vibration in the H-bonded NH. By a process of elimination, the band at 3429 cm^{-1} in NATMA(C) must be due to the ϕ-amide NH stretch. This suggests that the corresponding 3429 cm^{-1} band in NATA(B) and the 3430 cm^{-1} band in NATA(A) also be assigned to the ϕ-amide NH stretch. Based on this, the remaining 3416 and 3538 cm^{-1} transitions in the C5 structure, NATA(A) can be assigned as the ψ-amide NH_2 symmetric and antisymmetric stretch vibrations, respectively.

Returning to NATMA(A, B), we see that the 3440 and 3466 cm^{-1} bands in A have analogous transitions at 3431 and 3454 cm^{-1} in B, about 10 cm^{-1} below those in A. The two conformers are thus clearly spectrally distinct from one another, despite being similar in appearance. The 3431 cm^{-1} transition in NATMA(B) is very near the ϕ-amide NH stretches in NATMA(C), NATA(A), and NATA(B). We assign it as such, leaving the remaining 3454 cm^{-1} band of NATMA(B) as the ψ-amide NH stretch. The corresponding assignment for NATMA(A) places the ϕ-amide NH stretch at 3440 cm^{-1} and the ψ-amide NH stretch at 3466 cm^{-1}.

The vibrational bands in the 2800–3200 cm^{-1} region of Figs. 7 and 8 arise from CH-stretching vibrations, and are attributed to the CH-stretching modes of the indole ring and the peptidelike backbone. These transitions can be divided into three categories that arise from the following: (i) alkyl group vibrations (2900–3050 cm^{-1}); (ii) the ''phenyl'' side of the indole ring (3050–3100 cm^{-1}); and (iii) the pyrrole side of the indole ring (~3150 cm^{-1}). The spectra in this region show considerable congestion, as would be expected from the large number of CH groups present in the molecule. The phenyl CH stretch fundamentals (3050–3100 cm^{-1}) of NATA(A) [Fig. 7(a)] and NATMA(B) [Fig. 8(b)] are virtually identical to one another, but are quite distinct from that of the other three conformers. This suggests that NATA(A) and NATMA(B) are due to the same C5 conformer.

D. Assignment to individual C5 and $C7_{eq}$ conformers

Having made firm assignments of the NATA and NATMA conformers as C5 and $C7_{eq}$ structures, we next seek to assign particular C5 and $C7_{eq}$ structures to each NATA and NATMA species. Tables II and III summarize our assignments of the observed spectra to individual conformations of NATA and NATMA. The differences between the spectra of conformers that belong to the same family are more subtle than those that distinguish the families from one another. As a result, the assignments are somewhat more tentative, and are based on the combined evidence from a number of sources, which are summarized in this section.

In Sec. III A, the results of DFT Becke3LYP calculations for both NATA and NATMA were presented. These calculations identified four structures for each molecule that are calculated to be within 1 kcal/mol of the global minimum: two C5 and two $C7_{eq}$ structures (Fig. 3 and Fig. 4). There is very little change in the relative energies of these four conformers between NATA and NATMA, which only differ by the presence of a methyl group capping the ψ-amide NH in the latter molecule. One might anticipate on this basis that the number of conformers observed experimentally, and their relative populations, would not change significantly between

Downloaded 13 Jan 2003 to 131.111.112.171. Redistribution subject to AIP license or copyright, see http://ojps.aip.org/jcpo/jcpcr.jsp

TABLE III. A comparison of the calculated and experimental hydride stretch vibrational frequencies and infrared intensities of the three observed conformers of NATMA.

	NATMA A				NATMA B				NATMA C			
	Experimental frequency	Calculated frequency C5(AΦ)	Experimental intensity	Calculated intensity C5(AΦ)	Experimental frequency	Calculated frequency $C7_{eq}(\Phi P)$	Experimental intensity	Calculated intensity	Experimental frequency	Calculated frequency C5(AP)	Experimental intensity	Calculated intensity C5(AP)
Alkyl CH		2932		0.43		2928		0.58		2933		0.35
		2940		0.10		2933		0.22		2936		0.01
		2941		0.14		2941		0.13		2943		0.03
	2942	2959	0.29	0.26		2963		0.15		2947		0.15
		2989		0.05		2978		0.10		2985		0.12
	2980	3001	0.44	0.28	2977	2998	0.30	0.25		2995		0.04
		3011		0.07		3010		0.07		3011		0.02
	3003	3013	0.35	0.21	3003	3013	0.39	0.19		3018		0.08
		3041		0.08		3035		0.11		3026		0.10
Phenyl CH		3055		0.04		3055		0.02		3053		0.03
		3061		0.06	3057	3063	0.55	0.22		3058		0.02
	3073	3071	0.63	0.38		3072		0.09	3072	3069	0.66	0.17
	3094	3083	0.22	0.26	3073	3082	0.76	0.31		3081		0.13
Pyrrole CH		3135		<0.01		3132		0.01		3159		0.02
NH stretch	3440	3436	1.00	1.00	3431	3433	0.97	1.00	3344	3353	0.95	1.00
	3466	3464	0.67	0.49	3454	3466	1.00	0.76	3429	3446	1.00	0.60
	3522	3521	0.76	0.88	3522	3522	0.84	0.79	3523	3520	0.55	0.35

NATA and NATMA. However, the spectra of NATA can be accounted for entirely by two conformers (one C5 and one $C7_{eq}$), while there are three conformers of NATMA detected (two C5 and one $C7_{eq}$). We assume in what follows that the calculations have correctly identified the four lowest-energy structures, and look for distinctions between these candidates in making our assignments.

1. NATA

The assignment of NATA(A) to the C5(AP) structure and NATA(B) to $C7_{eq}(\Phi P)$ is based on the following evidence.

(a) The C5(AP) structure is 0.75 kcal/mol below C5(AΦ) while the $C7_{eq}(\Phi P)$ structure is 0.74 kcal/mol below $C7_{eq}(AP)$, after ZPE correction.

(b) The calculated frequency of the H-bonded NH stretch of the ψ-amide NH_2 group of NATA $[C7_{eq}(\Phi P)]$ is at 3340 cm^{-1}, very close to the experimental value of 3334 cm^{-1} for NATA(B). This match is better than with NATA $[C7_{eq}(AP)]$.

(c) The "free" NH stretch of the ψ-amide NH_2 group of $C7_{eq}(\Phi P)$ is predicted to be nearly degenerate with the indole-NH stretch at 3518 cm^{-1}, while the corresponding stretch in the $C7_{eq}(AP)$ conformer is predicted to be shifted farther to the red at 3512 cm^{-1}. The experimental spectrum for NATA(B) is a good match for the $C7_{eq}(\Phi P)$ conformer, as the asymmetric ψ-amide stretch is nearly degenerate with the indole-NH, with their experimental center frequencies at 3516 and 3521 cm^{-1}, respectively.

(d) The calculated CH stretch spectrum of C5(AP) matches NATA(A) remarkably well, particularly in the phenyl CH stretch region (3050–3100 cm^{-1}). The experimental intensity pattern in the transitions at 3059 and 3074 cm^{-1} is reproduced by the calculation and is characteristic of the C5(AP) structure.

(e) The relative intensities of the indole-NH and the antisymmetric ψ-amide NH-stretch at 3523 and 3538 cm^{-1} in NATA(A) more closely resembles the calculated intensities for C5(AP) than C5(AΦ).

(f) A weak vibronic structure in the LIF spectrum of NATA(A) appears at 20 and 41 cm^{-1} above the S_1-S_0 origin. The two lowest-frequency vibrational modes of C5(AP) have calculated harmonic vibrational frequencies of 23 and 39 cm^{-1}, while those for C5(AΦ) are at 18 and 32 cm^{-1}, a less satisfactory match.

2. NATMA

The C7 structure of NATMA is assigned to the same C7 conformer as in NATA; namely, $C7_{eq}(\Phi P)$. It is the lowest-energy C7 structure, has a somewhat better match with the frequencies and intensities of the observed NH stretch fundamentals, and is consistent with the assignment in NATA. There are two C5 conformers of NATMA observed. The evidence for assigning NATMA(A) as C5(AΦ) and NATMA(B) to C5(AP) is as follows.

Downloaded 13 Jan 2003 to 131.111.112.171. Redistribution subject to AIP license or copyright, see http://ojps.aip.org/jcpo/jcpcr.jsp

(a) The transitions due to NATMA(B) are more intense than those of NATMA(A) in the LIF spectrum, suggesting that NATMA(B) has a greater population, and hence is lower in energy than NATMA(A). The calculations place C5(AP) lower in energy than C5(AΦ) by 0.58 kcal/mol.

(b) The calculated intensity of the ψ-amide NH stretch fundamental is greater in NATMA[C5(AP)] than in NATMA [C5(AΦ)], consistent with the experimental intensities.

(c) The ϕ-amide NH stretch fundamental and the aromatic CH stretch transitions of NATMA(B) have the same intensity pattern and virtually identical frequencies to the corresponding transitions in NATA(A). This is consistent with the assignment of NATMA(B) to the same C5(AP) conformer assigned to NATA(A).

(d) The ultraviolet spectra of NATMA(A) and NATMA(B) possess Franck–Condon progressions involving modes with experimental frequencies of 12 and 24 cm^{-1}, respectively. The calculated lowest-frequency vibrations of C5(AΦ) and C5(AP) are 13 and 20 cm^{-1}, respectively.

IV. DISCUSSION

A. Conformational preferences of NATA and NATMA

The conformations of NATA and NATMA observed in the supersonic expansion belong solely to the C5 and $C7_{eq}$ conformer families. The lowest-energy C5 and $C7_{eq}$ structures are nearly isoenergetic, despite their very different dipeptide backbone structure. The C5 conformers have a dipeptide backbone that is extended in a nearly linear geometry that minimizes steric effects, and enables weak dispersive attractions with the indole ring. It occupies a position on the Ramachandran (ϕ, ψ) plot near that of a β-sheet secondary structure. The C7 conformers have a dipeptide backbone that contorts to form a seven-membered, H-bonded ring that joins the NH of one amide to the carbonyl of the other, in what could properly be called a γ turn.[30] Given the propensity of the individual amide groups to retain planarity, the formation of this intramolecular H bond introduces strain into the ring, which is compensated for by the stabilization of H bond formation. The end result is that the C5 and $C7_{eq}$ conformers are close in energy to one another in the gas phase.

Figure 9 shows an expanded view of the C5/$C7_{eq}$ branch of the disconnectivity graph of NATMA. The solid lines are the results that are obtained using the AMBER force field, including the calculated transition states binned with 0.5 kcal/mol resolution. The asterisks and dashed lines indicate the relative energies of the C5 and $C7_{eq}$ minima calculated using DFT Becke3LYP/6-31+G*. Clearly, there is qualitative, but not quantitative agreement between the two methods, as one might anticipate. It is encouraging that the AMBER force field agrees with the DFT B3LYP/6-31+G* results on which three conformers are lowest in energy: the C5(AΦ), C5(AP), and $C7_{eq}$(ΦP) conformers.

As with most tryptophan analogs, the $C_\alpha - C_\beta$ bond in almost all the low-energy conformations is roughly perpendicular to the indole ring. As a result, in NATA (NATMA), the N-acetyl and amide (methylamide) groups can take up positions anti, gauche on the phenyl side of indole, or gauche

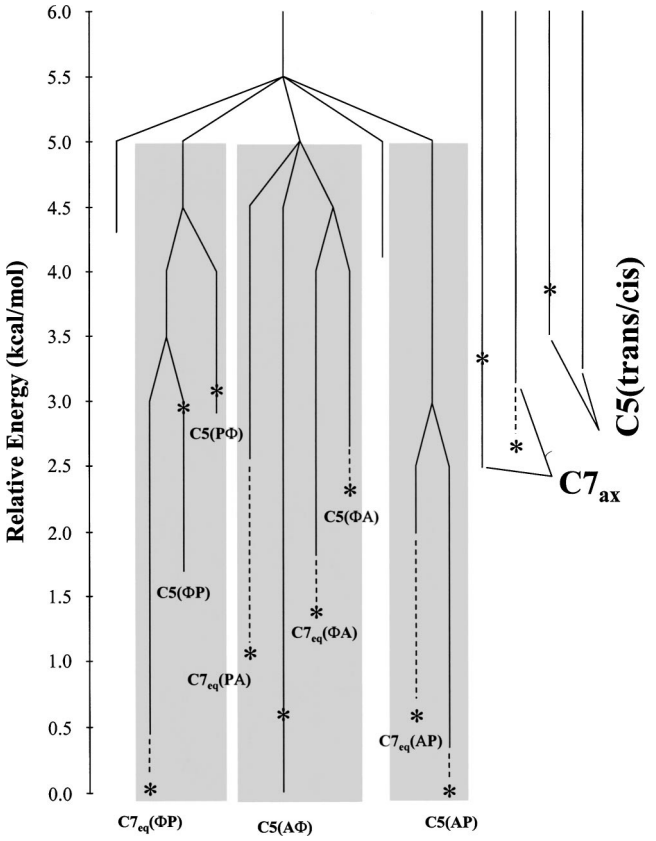

FIG. 9. Expanded view of the C5/$C7_{eq}$ *trans/trans* branch of the disconnectivity graph of NATMA, using a 0.5 kcal/mol bin size for the transition states. The solid lines give the relative energies of the conformers using the AMBER force field, while the dashed lines and asterisks locate the minima at the DFT/B3LYP 6-31+G* level of theory, including a zero-point correction. Note that 3 of the 12 C5/$C7_{eq}$ minima anticipated are not found by the AMBER force field. The unlabeled minima near the top of the diagram are not C5 or $C7_{eq}$ structures, but are connected to the low-lying C5 and $C7_{eq}$ structures by transition states near 5.5 kcal/mol.

on the pyrrole side of indole. With three positions and two groups, there are, in principle, a total of six C5 structures and six $C7_{eq}$ structures. Several of the conformers come in C5/$C7_{eq}$ pairs joined by a transition state of 3 kcal/mol or less. Of these 12 only the C5(PA) and $C7_{eq}$(PΦ) structures are not true minima on the surface, according to both DFT and AMBER calculations. In addition, the AMBER force field does not locate a minimum for the $C7_{eq}$(AΦ) structure. Of course, the DFT B3LYP calculations with a 6-31+G* basis set are not themselves truly benchmark calculations. DFT does not properly account for dispersion, and with the indicated basis set, intramolecular basis set superposition error is also non-negligible.

We have recently developed a technique called Population Transfer Spectroscopy (PTS), which is described in detail elsewhere,[31] that allows us to directly measure the ground state populations of the jet-cooled conformations. In the method, molecules are excited with a resonant IR pulse at a position in the expansion where collisions are still prevalent. These excited molecules conformationally relax over isomerization barriers, and are subsequently cooled to their zero-point levels via collisions with the bath gas (He) before being interrogated with an ultraviolet laser using LIF detec-

Downloaded 13 Jan 2003 to 131.111.112.171. Redistribution subject to AIP license or copyright, see http://ojps.aip.org/jcpo/jcpcr.jsp

tion. From an analysis of the changes in population of the conformers induced by the infrared laser as a function of infrared wavelength, we are able to determine the ground state, jet-cooled population distributions of the conformers detected in the LIF spectrum. The fractional ground state populations of the conformers of NATMA determined in this way are the following: $F_A = 0.23$ [C5(AΦ)], $F_B = 0.40$ [C5(AP)], and $F_C = 0.37$ [$C7_{eq}$(ΦP)].

On the one hand, the observed populations in NATMA are in fortuitously good agreement with the energy ordering and relative spacing of conformers A, B, and C predicted by the DFT calculations [E(B) = 0.00, E(C) = 0.07, and E(A) = 0.58 kcal/mol]. However, such a simple analysis of the observed populations in terms of the relative energies of the minima ignores entropic effects on the starting populations and the cooling of population out of higher-energy conformations that must necessarily occur in the expansion. Furthermore, the calculations predict four low-lying conformational minima for both NATA and NATMA: two C5 and two $C7_{eq}$, that come in C5/$C7_{eq}$ pairs of nearly identical energy. We would predict on the basis of energetics alone, either two or four structures, with no difference between NATA and NATMA. However, experimentally, NATA is observed to have two conformers with a significant population (one C5 and one $C7_{eq}$), while NATMA has three (two C5 and one $C7_{eq}$).

The populations downstream in the expansion are the net result of cooling an initial Boltzmann population of conformers thermally equilibrated at the nozzle temperature in a supersonic expansion. In order to quantitatively account for the populations observed downstream in the expansion, one must first of all have accurate calculations of the relative energies of all low-lying minima. The lowest-energy conformers identified by the calculations are likely candidates for maintaining their Boltzmann populations and for receiving additional population from higher lying minima. In the case of NATMA, the four structures shown in Fig. 4 are likely candidates for the observed conformations.

From the relative energies (after a zero-point correction) and vibrational frequencies of these minima, one must then calculate the relative free energies, from which the Boltzmann populations behind the nozzle can be determined. We have carried out such calculations on the low-lying conformational minima of NATMA, assuming harmonic vibrational frequencies for all normal modes taken from the DFT Becke3LYP calculations. Table IV summarizes the uncorrected and zero-point corrected relative energies and the relative free energies (calculated at the nozzle temperature of 423 K) of the different conformers of NATMA. The free energy calculations used the conformational energies and vibrational frequencies from the DFT calculations. According to the calculations, the three lowest-energy conformers account for about 75% of the population behind the nozzle, with the remaining 25% distributed among several higher-energy conformers that are not observed in the LIF spectrum. Note that the resulting relative free energies can differ by more than 2 kcal/mol from the relative energies of the minima. The difference in the entropies of the conformers forms the dominant contribution to these changes, and arises

TABLE IV. Uncorrected relative energies, zero-point corrected relative energies, and relative free energies of the ten lowest-energy minima calculated at the DFT Becke3LYP/6−31+GG* level of theory. All values are in kcal/mol.

Conformer	Relative energy (uncorr.)	Relative energy (ZPE corr.)	Relative free energy[a]	Lowest-energy barrier to isomerization[b]
$C7_{eq}$(ΦP)	0.00	0.07	2.28	2.58
C5(AP)	0.39	0.00	0.00	2.59
$C7_{eq}$(AP)	0.90	0.56	0.73	0.93
C5(AΦ)	0.96	0.57	0.65	4.60
$C7_{eq}$(PA)	1.45	1.07	1.32	2.44
$C7_{eq}$(ΦA)	1.55	1.30	2.10	2.19
$C7_{eq}$(AΦ)	2.59	2.23	2.61	[c]
C5(ΦA)	2.71	2.27	2.18	1.36
C5(ΦP)	3.51	2.94	2.83	1.32
C5(PΦ)	3.70	3.07	2.99	2.54

[a]The free energies are calculated at the nozzle temperature of 423 K.
[b]Isomerization barriers determined by the AMBER force field.
[c]This conformation was not a minimum in the AMBER force field.

almost entirely from differences in the frequencies of the low-frequency vibrational modes of the conformers. For instance, the $C7_{eq}$(ΦP) conformer of NATMA has both ''arms'' of the dipeptide over the indole ring, thereby stiffening the lowest-frequency vibrational modes (<100 cm^{-1}). This leads to a smaller entropy and pushes the free energy of this conformer about 2 kcal/mol up relative to the other low-lying conformers of NATMA. However, one must be careful not to put too much weight on such harmonic calculations, since the low-frequency modes are precisely those that are anticipated not to be accurately modeled by harmonic calculations.

Finally, if reliable initial populations of the highly populated conformers can be obtained, one must then understand how the pre-expansion populations are funneled into the observed minima during the expansion cooling process. When molecules are cooled rapidly in the supersonic expansion, the heights of the barriers that separate minima determine whether population is trapped behind the barriers or can be collisionally removed. Where that population ends up is determined by the connectivity of the potential energy surface; that is, by the way in which the higher-energy minima are connected to lower-energy minima on the potential energy surface. To illustrate this fact, the disconnectivity graph for NATMA shown in Fig. 9 reveals that the three observed conformers are the lowest-energy minima in each of three main ''branches'' enclosed in rectangles in the figure. One suspects then that the funneling of population into these three minima occurs because cooling occurs only inefficiently *between* these three main branches (which require overcoming barriers of ~5.5 kcal/mol according to the AMBER force field), but is efficient within a given branch, collecting all of the Boltzmann population within a given branch into the lowest-energy minimum in each branch.

While this provides a qualitative explanation for the observation of three conformers of NATMA, it does not resolve the question of why there are only two conformers of NATA observed. Recall that the NATA C5(AΦ) conformer is not

Downloaded 13 Jan 2003 to 131.111.112.171. Redistribution subject to AIP license or copyright, see http://ojps.aip.org/jcpo/jcpcr.jsp

observed, while the corresponding NATMA C5(AΦ) conformer accounts for 23% of the population downstream in the expansion. Evans and Wales have calculated a disconnectivity graph for NATA that is, not surprisingly, similar to that for NATMA, sharing with it the three branches to the low-energy region. However, the barriers separating the three branches are somewhat lower in NATA than in NATMA, hinting that perhaps these lower barriers allow the population to be funneled out of the C5(AΦ) branch during the cooling process.

In the past, studies of smaller molecules with fewer flexible degrees of freedom led to the rule of thumb that barriers of approximately 1000 cm^{-1} or higher (2.9 kcal/mol) are sufficient to trap the population behind them in a supersonic expansion.[32] An inspection of Table IV suggests that conformers of NATMA are overcoming barriers that are at least this size in a helium expansion. These rule of thumb arguments were based on the cooling of smaller molecules where the lowest-frequency modes are typically hundreds of wave numbers and the amount of internal energy stored in these modes is relatively small. Large molecules such as those studied here have many low-frequency modes below 100 cm^{-1} that possess kT of energy per mode under thermal equilibrium conditions prior to expansion. It is possible that the molecule uses this internal energy early in the expansion to overcome larger barriers to conformational isomerization. Furthermore, multiple pathways for isomerization can occur. Both may contribute to the efficient removal of populations from higher-energy minima. Realistic simulations of the cooling process would be helpful in better understanding the observed populations and their relationship to the pre-expansion Boltzmann distribution.

In summary, in order to understand the relative populations of large, conformationally flexible molecules downstream in a supersonic expansion, one must know a great deal about the potential energy surface beyond just which minima are the lowest in energy. Accurate relative energies for all low-lying conformational minima must be supplemented with analogous calculations on the transition states that connect them. These must in turn be linked into a connectivity diagram that assists in the determination of how population flows between conformational minima during cooling. Ultimately, better kinetic models of the collisional cooling in the expansion will also be required before a quantitative account can be made of the observed conformational populations when flexible biomolecules of this size are cooled in a supersonic expansion.

B. The unusual electronic spectroscopy of the $C7_{eq}$ conformers

Both NATA and NATMA use indole as their ultraviolet chromophore. As a result, the close proximity of the ^1L_a state to the ^1L_b state, which is thought to play an important role in the photophysics of indole, is also anticipated to play a similar role here.[33] In addition, the $^1\pi\sigma^*$ state is also likely nearby in energy, and may contribute to what is observed.[15] Both the ^1L_a and $^1\pi\sigma^*$ states have large dipole moments (albeit in opposite directions) that should be stabilized by polar environments. Thus, either of these states (or both of them) could get pulled down into the region of the ^1L_b state under certain circumstances.

The experimental fact is that, in both NATA and NATMA, the C5 conformers all exhibit a sharp vibronic structure and short Franck–Condon progressions involving low-frequency vibrational modes. In contrast, the $C7_{eq}$ conformers of both NATA and NATMA have a densely structured, red-shifted absorption without an identifiable origin transition. A broad intensity maximum in this structure occurs near the origins of the C5 conformers, but a long tail extends several hundred wave numbers to the red, and is replete with dense vibrational structure.

The qualitative interpretation of the unusual $C7_{eq}$ vibronic spectrum follows the line of reasoning laid out by Tubergen *et al.*[13] for the ^1L_a state, though it is equally applicable to the $^1\pi\sigma^*$ state. We assign the long tail to the red of the intensity maximum to a second electronic state that has shifted below the ^1L_b origin in the $C7_{eq}$ conformers. We ascribe the intensity maximum in the region of the C5 origins to the remains of the ^1L_b state, which is strongly coupled to a dense set of nearby vibronic bands due to the second state, so that the oscillator strength from the ground state to the ^1L_b origin is spread over many vibronic bands.

In order to test this qualitative explanation, LIF and FDIRS studies have been carried out on N-acetyl tryptophan ethyl ester (NATE). NATE differs from NATA and NATMA in that an ethyl ester group replaces the ψ-amide group. This substitution eliminates the possibility of forming an intramolecular hydrogen bond between amide groups, as in the C7 conformations of NATA and NATMA, and therefore restricts all the low-lying conformers of NATE to be C5 structures. The LIF spectrum of NATE is shown in Fig. 10. This spectrum agrees in every respect with previous LIF spectra of NATE by the Levy and Sulkes groups.[34,35] Park *et al.* identified S_1-S_0 origin transitions due to four conformational minima by power saturation studies.[34] These are labeled A–D in Fig. 10. We have confirmed these assignments by recording FDIR spectra of each of these conformers (not shown). While similar to one another, the FDIR spectra reveal small spectral shifts in the NH and CH stretch bands that confirm that there are four conformations that contribute to the spectrum of NATE. Furthermore, careful searches for a weak background in the LIF spectrum similar to that observed in NATA and NATMA revealed none. Thus, a close analog of NATA and NATMA that contains only C5 conformers also possesses only sharp vibronic transitions, providing further evidence that it is the C7 structure that is responsible for the changes observed in the vibronic spectra in NATA and NATMA.

Two issues remain. First, it is important to establish which state or states are responsible for the coupling: ^1L_a or $^1\pi\sigma^*$. Clearly, there is a need for further work, both experimental and theoretical, to try to understand the spectroscopic signatures and molecular-scale explanation for the extreme sensitivity of the vibronic spectrum on the conformation of the dipeptide backbone. We will report elsewhere on the S_1-state FDIR spectra of NATA and NATMA that point to-

Downloaded 13 Jan 2003 to 131.111.112.171. Redistribution subject to AIP license or copyright, see http://ojps.aip.org/jcpo/jcpcr.jsp

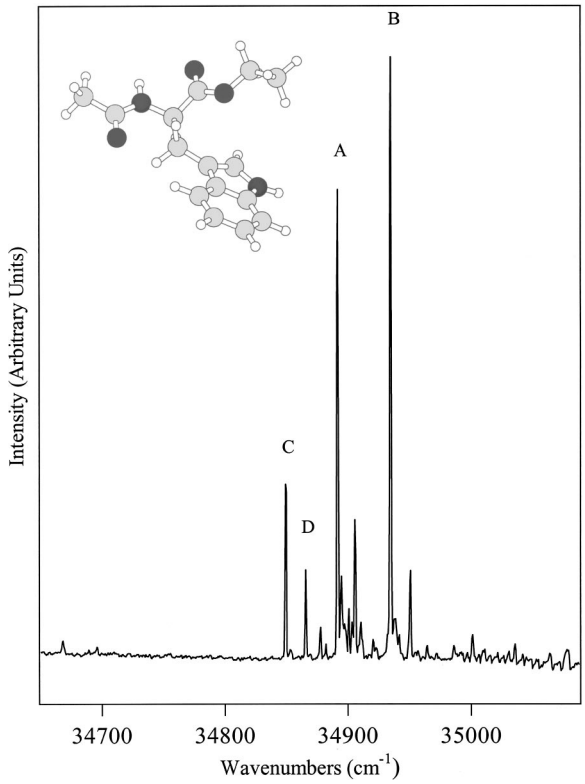

FIG. 10. LIF excitation spectrum of N-acetyl tryptophan ethyl ester (NATE) cooled in a supersonic expansion. The region near the S_1-S_0 origin is shown.

ward the $^1\pi\sigma^*$ state as the likely state responsible for the unusual electronic spectroscopy of the C7 conformers.

Second, we have not yet offered an explanation of *why* the $C7_{eq}$ dipeptide backbone structure would selectively lower the second state relative to ^1L_b, and why such a lowering is less pronounced or altogether missing in the C5 conformers. Given the large dipole moment of the $^1\pi\sigma^*$ (or ^1L_a) states, one might anticipate that the $C7_{eq}$ dipeptide backbone has a larger dipole moment that is configured so as to selectively stabilize the large dipole moments of the $^1\pi\sigma^*$ or ^1L_a states.[14] We have carried out calculations of the dipole moments of the C5 and $C7_{eq}$ backbones by substituting hydrogen for indole and keeping all else fixed. According to these calculations, the C5 and $C7_{eq}$ backbones have dipole moments that are similar in size (3.34 D versus 3.47 D). However, it may be not just the magnitude but also the direction of the dipole moment that is important. The $C7_{eq}$ structure has a substantial component of the backbone dipole moment ($\sim$1.2 D) that points in toward the indole ring, rather than parallel to it, as it is in the C5 structure. Alternatively, the selective stabilization of the ^1L_a or $^1\pi\sigma^*$ states may arise from aspects of the backbone charge distribution that cannot be properly captured by the dipole term alone. For example, in the conformers of interest, the amide NH often points in toward the indole π cloud, and forms a weak π H bond with it. The position and strength of this interaction may play an important role in the stabilization of the ^1L_a and/or $^1\pi\sigma^*$ states.[36] Such issues will be taken up further in a subsequent paper describing the S_1-state FDIR spectra of a series of indole derivatives.[37]

There is some indication that the state responsible for the unusual spectroscopy of the C7 conformers may not be far above ^1L_b, even in the C5 structures. All of the conformers (both C5 and $C7_{eq}$) show a sharp drop in fluorescence quantum yield just a few hundred wave numbers above the origin. This may indicate that the intruding state is lurking close by even in the C5 conformers; however, we have no direct evidence for this apart from the drop in fluorescence quantum yield.

If one can project from the dipeptides studied here to tryptophan-containing proteins in an aqueous solution, the sensitivity of the spectroscopy and fluorescence quantum yield to the conformation of the peptide backbone is rather starling, because it confirms that such large changes in the electronic spectroscopy can occur, even in the absence of interaction with a solvent.

ACKNOWLEDGMENTS

The authors gratefully acknowledge support for this research from the National Science Foundation under a two-year creativity extension to CHE-9728636, and the American Chemical Society Petroleum Research Fund (35988-AC6). The authors are grateful to Dr. H. Wang and Professor J. Chmielewski for their help in synthesizing NATMA. We also thank Professor P. R. Callis for helpful discussions about the excited states of NATA and NATMA. A.L. acknowledges the Ministerio de Ciencia Y Tecnologia for a post-doctoral fellowship. D.A.E. gratefully acknowledges financial support from the EPSRC.

[1] D. J. Wales, J. P. K. Doye, M. A. Miller, P. N. Mortenson, and T. R. Walsh, in *Advances in Chemical Physics*, edited by I. Priggogine and S. A. Rice (Wiley, New York, 2000), Vol. 115, p. 1.
[2] P. Derreumaux, Theor. Chem. Acc. **104**, 1 (2000); D. M. Standley, V. A. Eyrich, Y. L. An, D. L. Pincus, J. R. Gunn, and R. A. Friesner, Proteins: Struct., Funct., Genet. **5**, 133 (2001); J. A. Vila, D. R. Ripoll, and H. A. Scheraga, Proc. Natl. Acad. Sci. U.S.A. **97**, 13075 (2000).
[3] S. H. Gellman, Acc. Chem. Res. **31**, 173 (1998); I. Sack, Y. S. Balazs, S. Rahimipour, and S. Vega, J. Am. Chem. Soc. **122**, 12263 (2000); X. Fu and T. A. Cross, Magn. Reson. Chem. **36**, 651 (1998).
[4] E. Nir, C. Janzen, P. Imhof, K. Kleinermanns, and M. S. deVries, J. Chem. Phys. **115**, 4604 (2001); E. G. Robertson and J. P. Simons, Phys. Chem. Chem. Phys. **3**, 1 (2001).
[5] T. S. Zwier, J. Phys. Chem. A **105**, 8827 (2001).
[6] J. R. Carney and T. S. Zwier, Chem. Phys. Lett. **341**, 77 (2001); J. R. Carney and T. S. Zwier, J. Phys. Chem. A **104**, 8677 (2000).
[7] L. C. Snoek, E. G. Robertson, R. T. Kroemer, and J. P. Simons, Chem. Phys. Lett. **321**, 49 (2000); T. R. Rizzo, Y. D. Park, and D. H. Levy, J. Chem. Phys. **85**, 6945 (1986); L. A. Philips, S. P. Webb, S. Martinez III, G. R. Fleming, and D. H. Levy, J. Am. Chem. Soc. **110**, 1352 (1988); S. Martinez III, J. C. Alfano, and D. H. Levy, J. Mol. Spectrosc. **156**, 421 (1992); T. R. Rizzo, Y. D. Park, L. A. Peteanu, and D. H. Levy, J. Chem. Phys. **84**, 2534 (1986); L. C. Snoek, R. T. Kroemer, M. R. Hockridge, and J. P. Simons, Phys. Chem. Chem. Phys. **3**, 1819 (2001).
[8] M. D. Beachy, D. Chasman, R. B. Murphy, T. A. Halgren, and R. A. Friesner, J. Am. Chem. Soc. **119**, 5908 (1997).
[9] I. R. Gould, W. D. Cornell, and I. H. Hillier, J. Am. Chem. Soc. **116**, 9250 (1994); T. Head-Gordon, M. Head-Gordon, M. J. Frisch, C. L. Brooks III, and J. A. Pople, *ibid.* **113**, 5989 (1991); H. A. Stern, G. A. Kaminski, J. L. Banks, R. Zhou, B. J. Berne, and R. A. Friesner, J. Phys. Chem. B **103**, 4730 (1999).
[10] W.-G. Han, K. J. Jalkanen, M. Elstner, and S. Suhai, J. Phys. Chem. B **102**, 2587 (1998); C. D. Poon, E. T. Samulski, C. F. Weise, and J. C. Weisshaar, J. Am. Chem. Soc. **122**, 5642 (2000); P. E. Smith, J. Chem. Phys. **111**, 5568 (1999).
[11] O. M. Becker and M. Karplus, J. Chem. Phys. **106**, 1495 (1997).

Downloaded 13 Jan 2003 to 131.111.112.171. Redistribution subject to AIP license or copyright, see http://ojps.aip.org/jcpo/jcpcr.jsp

[12] W. D. Cornell, P. Cieplak, C. I. Bayly *et al.*, J. Am. Chem. Soc. **117**, 5179 (1995).
[13] M. J. Tubergen, J. R. Cable, and D. H. Levy, J. Chem. Phys. **92**, 51 (1990).
[14] L. S. Slater and P. R. Callis, J. Phys. Chem. **99**, 8572 (1995).
[15] A. L. Sobolewski, W. Domcke, C. Dedonder-Lardeux, and C. Jouvet, Phys. Chem. Chem. Phys. **4**, 1093 (2002); A. L. Sobolewski and W. Domcke, Chem. Phys. Lett. **315**, 293 (1999).
[16] A. L. Sobolewski and W. Domcke, Chem. Phys. Lett. **329**, 130 (2000).
[17] C. Dedonder-Lardeux, D. Grosswasser, C. Jouvet, and S. Martrenchard, Phys. Chem. Comm. **4**, 1 (2001).
[18] T. Walther, H. Bitto, T. K. Minton, and J. R. Huber, Chem. Phys. Lett. **231**, 64 (1994); T. Ebata, A. Fujii, and N. Mikami, Int. Rev. Phys. Chem. **17**, 331 (1998).
[19] M. Souhassou, C. Lecomte, R. H. Blessing, A. Aubry, M. M. Rohmer, R. Weist, M. Benard, and M. Marraud, Acta Crystallogr., Sect. B: Struct. Sci. **47**, 253 (1991).
[20] M. J. Frisch, G. W. Trucks, and H. B. Schlegel *et al.*, GAUSSIAN 98, Revision A.7 Gaussian, Inc., Pittsburgh, PA, 1998.
[21] F. Mohamadi, N. G. J. Richard, W. C. Guida, R. Liskamp, M. Lipton, C. Caufield, G. Chang, T. Hendrickson, and W. C. Still, J. Comput. Chem. **11**, 440 (1990).
[22] N. L. Allinger, J. Am. Chem. Soc. **99**, 8127 (1977).
[23] N. L. Allinger, Y. H. Yuh, and J.-H. Lii, J. Am. Chem. Soc. **111**, 8552 (1989).
[24] T. A. Halgren, J. Comput. Chem. **17**, 490 (1996).
[25] W. L. Jorgensen and J. Tirado-Rives, J. Am. Chem. Soc. **110**, 1657 (1988).
[26] S. H. Vosko, L. Wilk, and M. Nusir, Can. J. Phys. **58**, 1200 (1980); A. D. Becke, J. Chem. Phys. **98**, 5648 (1993).
[27] M. J. Frisch, J. A. Pople, and J. S. Binkley, J. Chem. Phys. **80**, 3265 (1984).
[28] J. R. Carney and T. S. Zwier, J. Phys. Chem. A **103**, 9943 (1999).
[29] G. N. Ramachandran and V. Sasisekharan, Adv. Protein Chem. **23**, 284 (1968).
[30] C. K. Mathews and K. E. v. Holde, in *Biochemistry* (Benjamin/Cummings, Redwood City, 1990), p. 171.
[31] B. C. Dian, A. Longarte, and T. S. Zwier, Science **296**, 2369 (2002).
[32] P. Felder and H. H. Gunthard, Chem. Phys. **71**, 9 (1982); R. S. Ruoff, T. D. Klots, T. Emilsson, and H. S. Gutowsky, J. Chem. Phys. **93**, 3142 (1990); P. D. Godfrey, R. D. Brown, and F. M. Rodgers, J. Mol. Struct. **376**, 65 (1996); P. D. Godfrey and R. D. Brown, J. Am. Chem. Soc. **120**, 10724 (1998); G. T. Fraser, L. H. Xu, R. D. Suenram, and C. L. Lugez, J. Chem. Phys. **112**, 6209 (2000); P. Butz, R. T. Kroemer, N. A. Macleod, and J. P. Simons, J. Phys. Chem. A **105**, 544 (2001).
[33] S. Arnold and M. Sulkes, J. Phys. Chem. **96**, 4768 (1992); P. R. Callis, J. T. Vivian, and L. S. Slater, Chem. Phys. Lett. **244**, 53 (1995); D. R. Demmer, G. W. Leach, and S. C. Wallace, J. Phys. Chem. **98**, 12834 (1994); B. J. Fender, D. M. Sammeth, and P. R. Callis, Chem. Phys. Lett. **239**, 31 (1995); R. J. Lipert, G. Bermudez, and S. D. Colson, J. Phys. Chem. **92**, 3801 (1988); K. W. Short and P. R. Callis, J. Chem. Phys. **108**, 10189 (1998); M. J. Tubergen and D. H. Levy, J. Phys. Chem. **95**, 2175 (1991); M. Vincent, J. Gallay, and A. P. Demchenko, *ibid.* **99**, 14931 (1995).
[34] Y. D. Park, T. R. Rizzo, L. A. Peteanu, and D. H. Levy, J. Chem. Phys. **84**, 6539 (1986).
[35] J. Sipior and M. Sulkes, J. Chem. Phys. **88**, 6146 (1988).
[36] P. R. Callis (private communication).
[37] B. C. Dian, A. Longarte, and T. S. Zwier (unpublished).

Downloaded 13 Jan 2003 to 131.111.112.171. Redistribution subject to AIP license or copyright, see http://ojps.aip.org/jcpo/jcpcr.jsp